An empirical correlation for burning of spruce wood in cone calorimeter for different heat fluxes

Paul Lardet, Alain Coimbra, Lucas Terrei, Elmehdi Koutaiba, Renato Mole-Antoniazza, Gabriel Giovannelli

An empirical correlation for burning of spruce wood in cone calorimeter for different heat fluxes

Paul Lardet, Alain Coimbra, Elmehdi Koutaiba, Renato Mole-Antoniazza and Gabriel Giovannelli : CSTB (Centre Scientifique et Technique du Bâtiment (CSTB), Université Paris-Est, Champs-sur-Marne, France)

Lucas Terrei : LEMTA (CNRS, LEMTA, Université de Lorraine, 54000 Nancy, France)

Abstract

This article proposes an empirical expression to describe the pyrolysis and charring of spruce wood in bench-scale experiments for a wide range of incident heat fluxes. Spruce wood samples were exposed to a cone radiant heater oriented vertically with varying intensities, ranging from $\dot{q}_{\text{cone}} = 22$ to 93.5 kW m^{-2} over 53 test samples. The mass loss rate (MLR), the position of the char front and a preliminary additional heat source from smoldering or flaming combustion were experimentally determined. The experimental data were processed to express the burning rate as a function of heat flux and char front position. A grouping of the experimental curves was obtained, allowing to predict the MLR outcome over time regardless of the incident heat flux. A linear regression at the quasi-steady state regime allowed the determination of the fitting coefficients of the correlation, which ultimately correspond to the mass of volatiles produced per unit of energy input into the material. A comparison was made with theoretical analysis of the pyrolysis of charring materials from the literature, and the discrepancies with the proposed approach and its limitations were finally discussed. The main advantage of this approach is that it provides a generalized expression, requiring minimal input of material properties, which predicts the MLR change over time for any heat flux within engineering accuracy.

Keywords: Wood degradation, Mass loss rate, Cone calorimeter, Spruce wood, Pyrolysis, Material flammability

1 Introduction

The use of engineered timber products has been steadily increasing in a variety of multi-story residential and commercial buildings in recent years. Their environmental and aesthetic features, as well as their favorable strength-to-weight ratio make them an appealing solution in comparison to concrete or steel [1]. A common material applied for these purposes in Europe is spruce wood. However, its flammability constitutes a major drawback for these applications [2, 3]. In order to mitigate the fire risks posed by these materials, it is necessary to be able to predict their pyrolysis behavior when exposed to heat flux, which is directly related to their propensity to sustain and

propagate flames [4–7]. Their thermal response could then be implemented in larger-scale CFD engineering models, which are well suited for simulating flame spread and fire growth.

With that purpose, numerous studies have been carried out over the last few decades to model the pyrolysis of charring solids [8–10]. These range from analytical expressions with many simplifying assumptions [11–13] to complex systems of coupled partial differential equations describing heat and mass transfer through wood and char, chemical decomposition, smoldering and flaming combustion, etc [14–16]. Simple theoretical models provide insight on the key parameters and material properties that influence the pyrolysis and charring processes. However, their simplifying assumptions often result in inaccurate predictions of the solid mass loss rate, charring rate and char depth under varying thermal exposures and experimental configurations [9]. Comprehensive pyrolysis models, on the other hand, can effectively correlate the material properties to their thermal decomposition behavior, through physics-based descriptions of in-solid heat and mass transfer and simplified chemical processes. They require however the development of a reaction model as well as a large amount of material property input. These apparent properties include but are not limited to kinetics, thermodynamics, heat and mass transport related parameters, char porosity and permeability. Due to the coupled nature of the processes involved, these parameters are often not directly measurable and the range of validity of the model may be limited to the conditions that were used during their calibration [17].

In order to circumvent these difficulties, a third family of pyrolysis models is often used in fire safety engineering applications. These models are based on the empirically-observed proportionality between the incident heat flux and the solid degradation, predicting the MLR in a simple and cost-effective approach [18, 19]. A major limitation of this group of studies is the often poor prediction of the MLR, especially in the initial complex transient regime commonly found in charring solids degradation.

With the aim of improving the accuracy of wood degradation prediction in fire safety engineering and modelling, this paper proposes a novel solution for calculating the burning rate of spruce wood. It consists on the development of an empirical expression based on the treatment of experimental data from cone calorimeter tests. It is shown how these complex phenomena can be empirically translated into a simple expression that correlates the solid burning rate to the char front position and the incident heat flux. The novelty of this work relies on providing a novel point of view on how to approach the material burning rate in real engineering situations.

The article is organized as follows. The experimental procedure and materials are described in section. 2. The experimental results obtained with the cone calorimeter are also reported. Section. 3 describes the treatment of the experimental data which enables development of the empirical expression. The development of the correlation and fitting of its coefficients are then performed in section. 4. A discussion of the results is done in section. 5, as well as a comparison with theoretical work from the literature. The final comments and remarks are drawn in section. 6.

	Cone heat flux (kW m^{-2})					
Property	22	38.5	49.5	60.5	82.5	93.5
Replicated experiments (-)	3	2	7	3	3	3
Average density (kg m^{-3})	516.7	530.7	454.8	507.3	492.3	457.7
Average residual mass (g)	158.7	132.3	86.3	53	36	28.3
Residual char front position (mm)	26	33	39.6	47.5	49.8	50

Table 1 Properties of spruce wood samples.

2 Experimental methodology

The materials, test samples, experimental setup and methods are briefly described in this section. A more extensive description of these subjects can be found in previous works [20, 21].

2.1 Materials and methods

The material considered in this work is spruce wood in the form of Glue Laminated Timber (Glulam). The samples were cut in 100 mm × 100 mm in size, with a thickness of 50 mm. The thickness of the specimen and the position of the adhesive layer were chosen so that it could be considered as a semi-infinite sample. Six sets of tests are considered in this study, with a total of 21 used samples (for the complete experimental test). The moisture content of the samples was measured between 9 and 11 %. It was observed that, in this range, the moisture content did not have a significant effect on the measured MLR values [20].

The experimental setup is illustrated in Fig. 1. The tests were performed with a cone calorimeter oriented vertically [22]. The samples were wrapped with two layers of aluminum foil, except their top side exposed to the radiative flux, and the distance between the sample and the heater was 25 mm. Radiative heat fluxes emitted by the cones were controlled before each test by using a Schmidt-Boelter fluxmeter (by Medtherm). The heat flux was considered correct when the value was ±0.5 kW m^{-2} from the desired flux. In this study, the samples were exposed perpendicularly to the wood grain, with a constant heat flux of $\dot{q}''_{\text{cone}}$ = 22, 38.5, 49.5, 60, 82.5 and 93.5 kW m^{-2}. The cone data reported in this work are the average of replicated experiments. The total number of experimental sets were 53 (21 for complete tests and 32 for measuring char layer depth in specific durations of the test). The individual and unfiltered tests are shown in the appendix of the manuscript. The mean and filtered value (smoothing was based on averaging experimental data over 30-second intervals.) that is used for the rest of the manuscript is also shown as dashed, black lines. Good repeatability is observed between the tests, notably in the time and magnitude of the peak MLR." Each sample property and details are presented in Table 1.

The cone calorimeter was used initially to determine the solid mass loss rate per unit area (referred to as MLR hereafter) evolution with the time, with each test lasting at least 60 min. The position of the char front e (or pyrolysis front) was also measured at specific instants for each test setup. These additional tests were interrupted at different durations and then rapidly cooled with liquid nitrogen in order

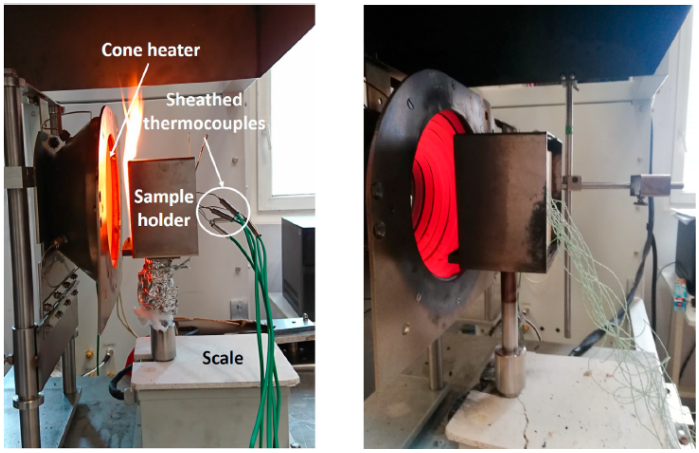

Fig. 1 Experimental setup of the vertical cone calorimeter [21].

to stop pyrolysis reactions. The samples were cut in the middle of their cross-sections and the char front was measured with a ruler.

The in-depth temperatures were also measured, by embedding twelve thin (0.1 mm diameter) wire thermocouples inside the sample. The wires were thin and supple enough so that mass loss and temperature in the solid can be simultaneously measured. The base of the charring layer is widely accepted to be between $280 < T < 300$ °C [23, 24]. By tracking the isotherm $T = 300$ °C the position of the pyrolysis front (considered as the char front) could be determined. Details and discussions about these processes, as well as comparisons with char front measurements using the two methods can be found in ref. [21].

A major difficulty in the determination of the total incident heat flux perceived by the solid is the identification of smoldering and flaming ignition and their contributions as an additional heat source [25] ($\dot{q}''_{\text{inc}} = \dot{q}''_{\text{cone}} + \dot{q}''_{\text{flame}} + \dot{q}''_{\text{smoldering}}$). The flaming heat fluxes $\dot{q}''_{\text{flame}}$ in an horizontal orientation were previously found to be between 20 (peak value) and 2 kW m^{-2} (steady-state value) in the Fire Propagation Apparatus [26]. In the experimental device used in this work, one can expect smaller heat flux values, due to the smaller size of the samples and the flames distribution over the samples. For smoldering combustion, a preliminary attempt has been conducted to quantify the resulting heat contribution to the solid degradation. This contribution was estimated by conducting tests with a cone calorimeter using a controlled atmosphere chamber. First, a sample of spruce wood was exposed vertically to 16.5 kW m^{-2} without an igniter for 40 minutes. There was no ignition, and it was possible to observe the transition between pyrolysis and pyrolysis coupled with smoldering. This resulted in an initial plateau of MLR and surface temperature (pyrolysis), followed by an increase in MLR and surface temperature (measured by an IR camera) until reaching a second plateau when the entire wood surface was incandescent. Following this experiment, the sample was placed in an inert atmosphere chamber where only pyrolysis could occur, so no transition to a second plateau due to smoldering was observed. The heat flux from the cone that allows reaching this second plateau observed in air tests was

determined to be approximately $\dot{q}''_{\text{smoldering}} = 11$ kW m^{-2}. Further details about this process may be found in ref. [20]. The resulting value is consistent but larger than the result of previous work [26]. It is important to notice that this work was exploratory and experiments for other heat fluxes need to be carried out. Only fine modeling of solid combustion would make it possible to precisely explain the additional flux generated for each heat flux, and how it is affected by flaming combustion and vice-versa.

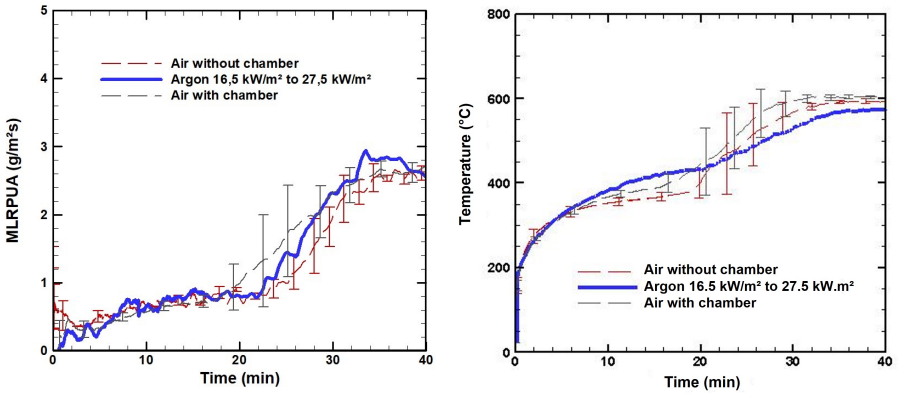

Fig. 2 Comparison of MLR and surface temperatures based on experimental conditions for characterizing the additional heat flux generated by smoldering combustion: Mass loss rate (left) and surface temperature (right). Extracted from [20].

2.2 Experimental results

The experimental MLR obtained from cone calorimeter experiments at different heat fluxes is shown in Fig. 3. As the cone radiative heat flux is increased, the time to ignition and the burning duration decrease while the peak MLR increases. The sample burning behavior is nevertheless similar for all six cases. Pyrolysis starts rapidly (a few seconds after the start of the test) and is followed by a rapid increase (except for the lowest heat fluxes) in the MLR up to a short peak (between 1 and 2 minutes). When exposed to the lowest heat fluxes (22 kW m^{-2}, 38.5 kW m^{-2} an to a lesser extent 49.5 kW m^{-2}), flaming ignition may not occur, or it occurs after a long time (up to 50 min). In these cases, smoldering ignition occurs before the flames appeared (from 2 to 12 minutes). For this reason, a less pronounced MLR peak is observed in the initial phase, as the thermal impact of flaming combustion on the virgin, uncharred wood surface is less pronounced. For all cases, a char layer of significant thickness starts to be formed after heat exposure begins, which inhibits the degradation of the wood by slowing down heat and mass transfer between the gaseous and condensed phases and thus protecting the substrate material [25]. The MLR then reaches a quasi-steady-state behavior, with a steady decrease over the test. At the later phases of the process (between 50 and 60 min, for the higher heat fluxes) the material burning decreases rapidly until extinction. This phase corresponds to the instants when the

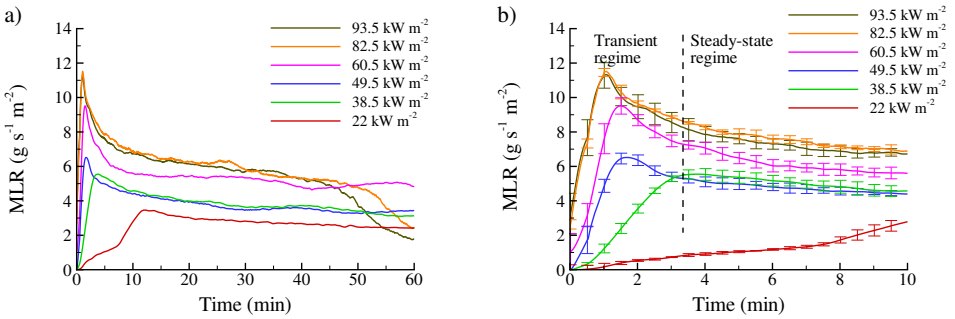

Fig. 3 (a) Experimental MLR evolution of spruce-wood samples at different heat fluxes. (b) Detail of the MLR at the initial transient stages with error bars.

wood is almost entirely carbonised. The thermally thick assumption is therefore no longer valid, and these periods are excluded from the analyses of this study.

The experimentally determined char front position progression, measured from the visual method, is given in Fig. 5. It suggests, as expected, that along with the increased MLR, the char front advances quicker with the higher heat fluxes. This behavior is qualitatively consistent with previous studies conducted for other wood species [18]. The charring rate can also be inferred from the slopes of the char front position progression with the time, although only approximately inferred due to the lack of experimental points using the visual method. The charring rate was found to reach a peak value around 2.0 mm min^{-1} in the transient parts, for the heat fluxes of $\dot{q}''_{\text{cone}} = 60.5$ and 93.5 kW m^{-2} and to decrease to a quasi steady state around 0.7 mm min^{-1} (see Fig. 4). For the lowest heat fluxes, the charring rate at 20 min of test start (steady state regime) was found to be around 0.4 and 0.6 mm min^{-1} for the heat fluxes of $\dot{q}''_{\text{cone}} = 22$ and 38.5 kW m^{-2}, respectively. These values are in accordance with measurements and empirical models in the literature [27].

3 Results analysis

From the analysis of Figs. 3 and 4, a similar behaviour can be observed between the MLR and the char front positions in terms of their imposed cone heat fluxes. By assuming that the pyrolysis process occurs in an infinitesimally thin sheet, and that it happens much faster than other heat and mass transport phenomena [28], the correlation between the MLR, $\dot{m}''$, and the derived char front e can be expressed as:

$$\dot{m}'' = \dot{e} \cdot \rho_v = \dot{e} \cdot \rho_0 \cdot (1 - \tau_c), \tag{1}$$

where ρ_v is the density of pyrolysable material in the wood, ρ_0 is the density of the initial, virgin wood sample and τ_c is the char fraction. Under the aforementioned assumptions, quantifying the pyrolysis rate is equivalent to quantifying the rate of advance of the char front.

The char fraction is defined as the char density divided by the initial, virgin wood density. At the end of a cone calorimeter test ($t = 60$ min), the remainder of the

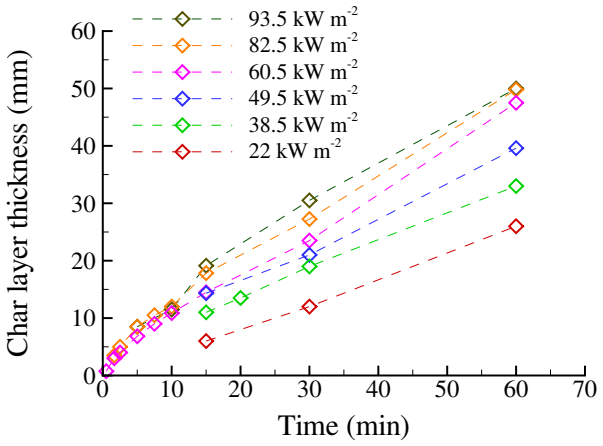

Fig. 4 Experimentally measured char front position using the visual method at different cone heat fluxes [21].

sample was weighted and its dimensions recorded (see Table. 1). Assuming that the density and height of the post-test virgin wood remain constant during the test [13], the char fraction is obtained as a geometric correlation between initial and final sample properties:

$$\tau_c = \frac{1}{\rho_0}\left(\frac{m_f - \rho_0 A_0(\eta_0 - \eta_{c,f})}{A_0 \eta_{c,f}}\right), \tag{2}$$

where A_0 is the sample surface area, m_f is the final sample mass and η_0 and $\eta_{c,f}$ are the initial sample thickness and final char layer depth, respectively. The average sample char fraction was not found to be constant for different heat fluxes. Indeed, it seemed to increase as the incident heat flux decreased, and a local char fraction also appeared to decrease with time throughout the cone calorimeter test. It has been suggested by Lyon et al. [29] that it can be a function of temperature. The moisture content of the sample could also affect the resulting calculation of the char fraction [30]. Further investigation of the char fraction was not a subject of this article. For the rest of this study, the largest calculated char fraction, i.e., the average char fraction obtained for the smallest cone heat flux sample of $\tau_c = 0.26$ will be used as a safety factor.

By using Equations 1 and 2, the charring rate is calculated for each set of experiments. For the cone heat fluxes of $\dot{q}''_{\text{cone}} = 60.5$ and 93.5 kW m^{-2}, the calculated charring rate is depicted in Fig. 5. Only average values of the experimental sets are shown. Reasonably good agreement with both experimental data methods is observed in the transient phase. At later stages ($t > 10$ min) the calculated charring rate exceeds the experimentally measured values, especially for the higher cone heat fluxes. This may be due to the thermally thick assumption being no longer valid for those cases, as well as the safety margin given in the calculation of the mean char fraction, deducted from the cone heat flux of $\dot{q}''_{\text{cone}} = 22$ kW m^{-2}.

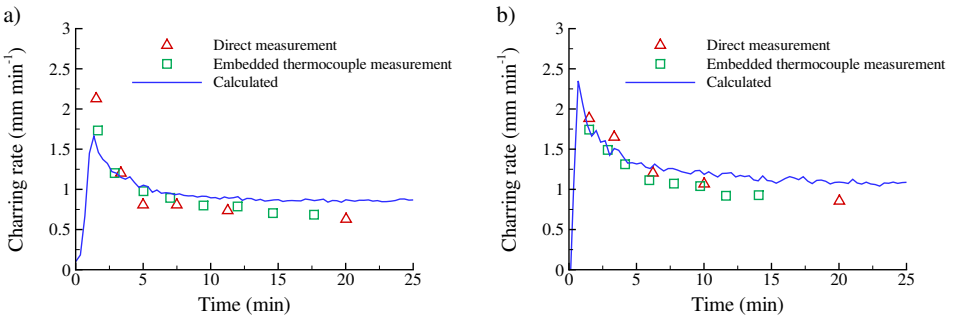

Fig. 5 Experimentally measured [21] and calculated charring rates (a) $\dot{q}''_{\text{cone}} = 60.5$ kW m^{-2}. (b) $\dot{q}''_{\text{cone}} = 93.5$ kW m^{-2}.

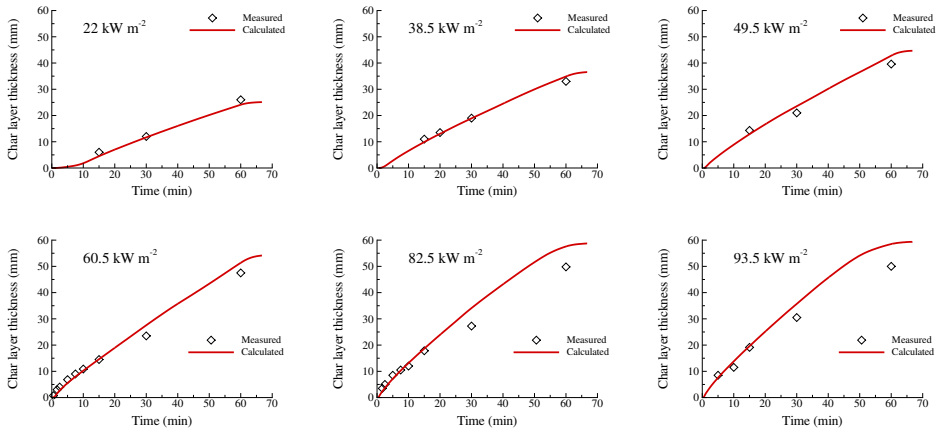

Fig. 6 Experimental and calculated char front position at different radiant heat fluxes.

The charring rates are next integrated over time in order to obtain the position of the char front for each replicated experiment and heat flux. The average calculated values of the char front positions are shown in Fig. 6. Experimentally measured data using the visual method are also displayed, showing good agreement with the proposed methodology for a wide range of heat fluxes. At the end of the experiment, the calculated values slightly exceed the measured ones as the external heat flux increases. This shows the difficulty of accurately defining a single char fraction value, as well as in interpreting the MLR once the sample is almost entirely carbonised and the thermally thick assumption is no longer valid. A similar analysis of the calculation of char layer thickness from the MLR has been presented in refs.([31, 32]).

The objective is to predict the mass loss behavior of the sample regardless of the incident heat flux and char front position. With that purpose, the MLR is normalized by the incident heat flux corrected by considering a complementary heat source including smoldering and flaming combustion contribution, $\dot{q}''_{\text{tot}} = \dot{q}''_{\text{cone}} + \dot{q}''_{\text{combustion}}$.

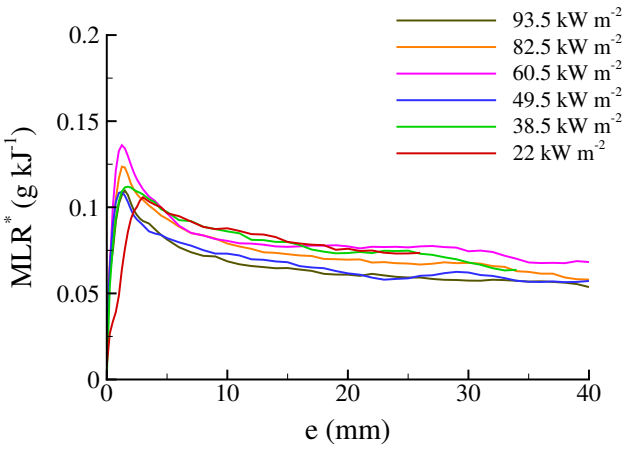

Fig. 7 Mean MLR* for each incident heat flux as a function of the char front position.

As a simplifying assumption, the present work chooses a unique value of $\dot{q}''_{\text{combustion}} = 10\ kW\ m^{-2}$ as a combined smoldering and flaming combustion contribution. A precise detection and quantification of these processes as a function of the incident heat flux is numerically and experimentally difficult, and is largely dependent on each individual sample, as well as many other factors. In order to stay faithful to a robust and reliable engineering approach, this simplifying assumption must be used at this stage. This value is consistent with the one calculated in [26]. The resulting curves with the normalized $MLR^* = \frac{MLR}{\dot{q}''_{\text{tot}}}$ are shown in Fig. 7. This proposed treatment enables a grouping on the x and y axis of the MLR^*, for a wide range of incident cone heat fluxes.

4 Correlation

The proposed experimental treatment approach seems to confirm the possibility to express the MLR as a function of the heat flux and charring front position. The methodology to formulate a correlation is presented in this section in the form of:

$$MLR = \dot{q}''_{\text{tot}} \times MLR^*(e). \tag{3}$$

This approach is equivalent to an x and y axis correction of the mass loss rate or heat release rate versus time given a reference experimental set of cone calorimeter data. This kind of approach has been recently implemented in the latest version of the fire modelling package Fire Dynamics Simulator (FDS version 6.8.0, "scaling the burning rate by the heat flux") [33, 34]. Validation works using a large amount of materials available in public datasets seemed to support the robustness of this method. However, to the knowledge of the authors, this solution is purely mathematically based. The present work seeks to give thermal analysis and interpretation that supports

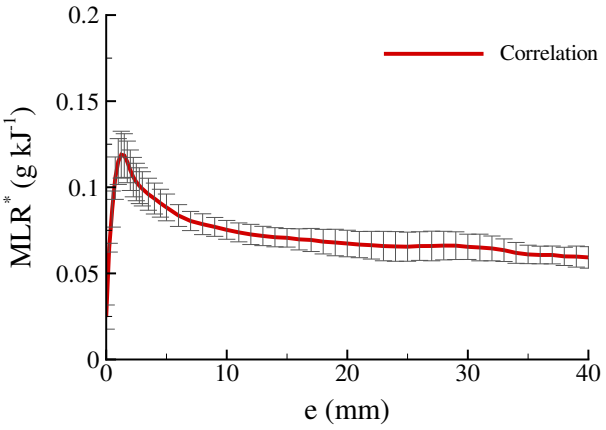

Fig. 8 Mean normalized MLR as a function of the char front position for cases with flaming and smoldering combustion.

this scaling factor by correlating the burning rate to the charring rate and char front position.

A mean value of MLR* only depending on char layer depth for all heat fluxes is used to build this correlation, shown in Fig. 8. Two regimes can be distinguished: an early, low char thickness, regime with a strongly transient behavior, and a late, high char thickness, regime with a quasi-steady state behavior. The standard deviation is also displayed, showing that with the proposed treatment the curves become very close to each other for various heat fluxes, even for those with non-flaming combustion. The empirical correlation can therefore be formulated in an uncoupled way, i.e., regardless of the imposed heat flux value.

Where char layer depth $e > 5\ mm$ (quasi-steady state regime), this work proposes a formulation of Eq. 3 in the form of:

$$MLR^* = \frac{a}{e} + b. \tag{4}$$

As an engineering method, this work supposes that the coefficients to be determined a and b are independent of the imposed heat flux. This approach is chosen based on empirical observation, with the intention of providing a determination of the MLR in a robust model whatever the imposed heat flux. In the analytical analysis of wood combustion, it has been reported that these coefficients may not be independent of the incident heat flux in a thermal analysis perspective [13]. A physical interpretation of these coefficients will be discussed in section 5.1.

The treated MLR* is represented as a function of $1/e$ in Fig. 9 where $e > 5$ mm. Only values of char front position greater than 5 mm are represented, which correspond to the quasi steady-state regime. A linear tendency between the terms is indeed observed, and linear regression allows the determination of the sought parameters, given in Fig. 8. An expression for Eq. 4 during the quasi-steady state regime can be formulated:

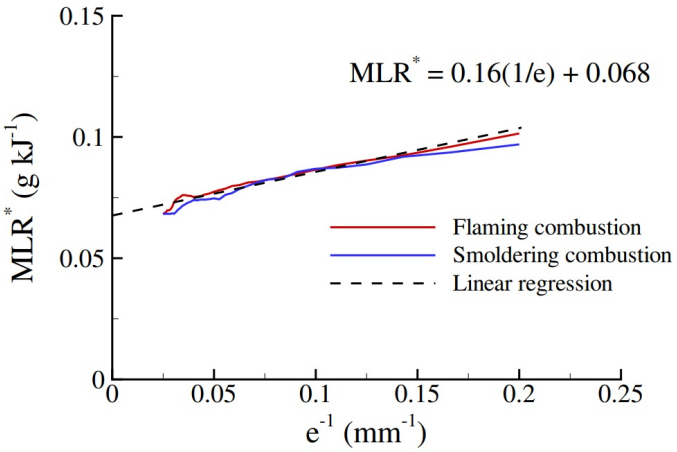

Fig. 9 Linear regression of MLR* as a function of $1/e$.

$$MLR^* = \frac{0.16\left[\frac{\text{g mm}}{\text{kJ}}\right]}{e} + 0.060\left[\frac{\text{g}}{\text{kJ}}\right]. \tag{5}$$

Finally, Eq. 3 is used to reproduce the MLR for different heat fluxes in Fig. 10. MLR^* is tabulated from mean grouped experimental data where $e < 5$ mm and calculated from Eq. 5 where $e > 5$ mm.

The final correlation is shown to accurately represent the experimental data for a wide range of incident heat fluxes. The correlation is found to slightly over-predict the values for the highest cone heat flux. This was indeed expected, as the results for $\dot{q}''_{\text{cone}} = 82.5$ and 93.5 kW m^{-2} were nearly identical, and a plateau of the resulting MLR seemed to be reached for these experimental settings, independently of the increased incident heat flux beyond this point. The transient peak regime was not well predicted for the two lowest heat fluxes. The initial peak in these cases is less prominent than in the highest heat flux cases cases, which could suggest that the flame heat flux is not constant in the initial phase, and it could play a major role in the resulting MLR. A detailed understanding of the heat flux contributions to this initial phase would require more experimental data and modeling.

The Eq. 1 and Eq. 3 and the curve from Fig. 8 are finally used to compute the MLR as a function of the time.

$$\dot{e} \cdot \rho_0 \cdot (1 - \tau_c) = \dot{q}''_{\text{inc}} \times f(e). \tag{6}$$

Eq. 6 is solved using a forward Euler scheme. This was done for verification purposes. The correlation could be implemented in a simulation software using more sophisticated schemes.

1. At the instant t_0, the char front position is initialized with $e_0 = 0$. t_0 is the time when the pyrolysis process starts.
2. At any instant t_n, the MLR is calculated from Eq. 3 with e_n and $\dot{q}''$.
3. Then the charring rate $\dot{e}_n$ is determined from Eq. 1.

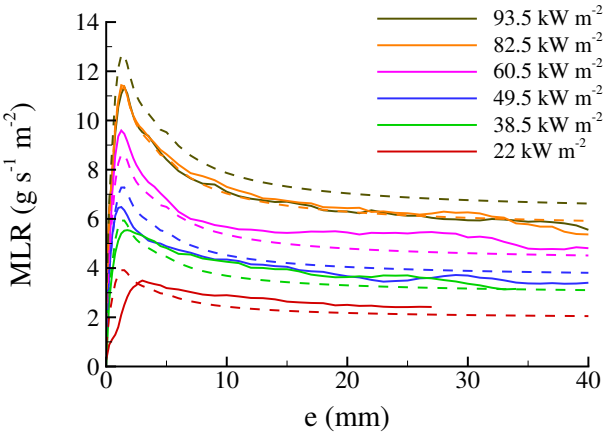

Fig. 10 Mean experimental and calculated MLR as a function of the char front position (a) Heat fluxes with flaming combustion; (b) Heat fluxes with smoldering combustion.

4. The char front position at the next time step t_{n+1} is obtained from integrating $\dot{e}_n$ between t_n and t_{n+1}, i.e., $e_{n+1} = e_n + \int_n^{n+1} \dot{e_n}\, dt$.
5. The MLR at instant $n+1$ is again calculated as in step 2.

This process is schematized in Fig. 12.

Results are presented in Fig. 11. Again, the overall agreement with the experimental results is remarkable. It is also shown from Fig. 10(b) that this approach successfully predicts the temporal shift in time of the MLR peak at the transient regime, caused by the increase or decrease of $\dot{q}''_{\text{cone}}$. This is a major enhancement compared to the results obtained with a simple model of MLR only proportional to the heat flux [19].

The given correlation can be easily implemented in a flame spread and fire growth model. An overall summary of the development of the correlation is schematized in Fig. 12. The experimental MLR data is used to compute the char fraction and the charring rate from Eqs. 2 and 1. An integration with the time allows for determination of the char front position at each instant t. The MLR is divided by the experimental heat flux input becoming MLR*, which can be now plotted a function of e. The correlation appears from the grouping of the experimental treated curves. For the quasi steady-state regime, linear regression of the curve allows for the description of the coefficients presented in Eq. 5.

5 Discussion

5.1 Analytical formulation and thermal analysis

While the correlation presented in the last section is entirely empirical, the resulting coefficients a/e and b correspond, from a thermal perspective, to the inverse of the enthalpy of pyrolysis. This means that these parameters, expressed in $\left[\frac{\text{g}}{\text{kJ}}\right]$, can be interpreted as the mass of pyrolysis gases produced per unit of energy input.

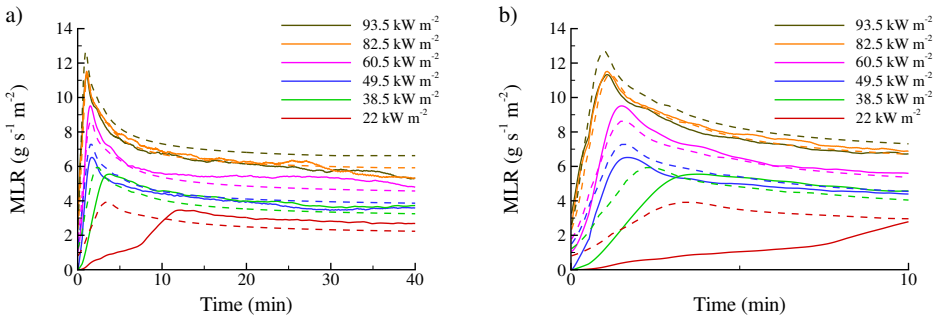

Fig. 11 (a) Mean experimental and calculated MLR as a function of the time; (b) Detail at the initial transient stages.

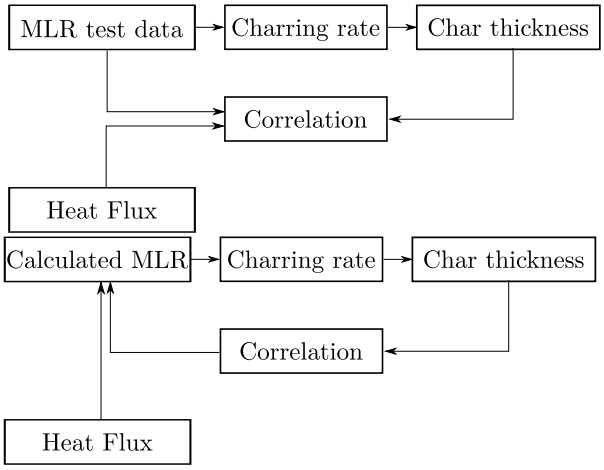

Fig. 12 Top: Flowchart describing the development of the correlation from the experimental data. Bottom: Flowchart describing the application of the correlation for obtaining the calculated MLR.

In a qualitative thermal analysis conducted by Spearpoint and colleagues on the burning rate of solid materials [13, 28] it has been suggested that this quantity, denoted as the steady state heat of gasification, should reduce to zero when the char front position increases. This suggests, from a thermal analysis perspective, that the b term from Eq. 4 should be equal to zero and the MLR should therefore approach zero when time increases. This tendency is however not observed on the experiments performed on spruce wood in this work, as well as for other wood species reported in the literature [35]. In the work of Spearpoint et al. (2000) [13], cone calorimeter experiments reported that this effect is also not experimentally observed. For example, Fig. 13 shows results for Douglas fir samples. As a consequence, a theoretical prediction based on simplified thermal analysis leads to an under-prediction of the burning rate. The b term from Eq. 4 could be then interpreted as a permanent regime term. Many factors could explain the origin of this compensatory factor, such as other heat transfer mechanisms

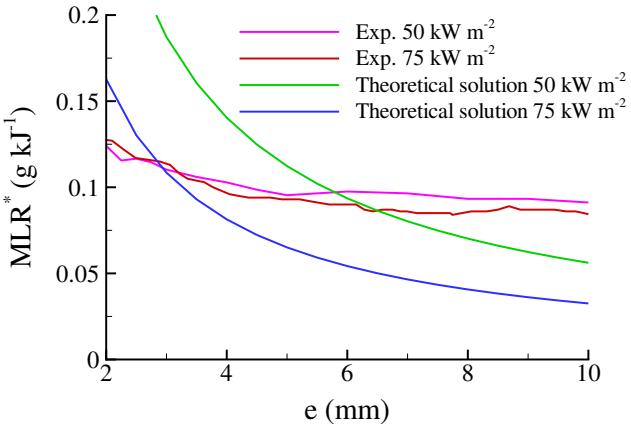

Fig. 13 MLR* as a function of the char front position: theory and experimental data for Douglas fir sample at $\dot{q}''_{\text{cone}} = 75$ kW m^{-2} from Spearpoint et al. [13].

of a convective or radiative nature across the char after surface regression and cracking during the burning process [23, 36].

Furthermore, in the thermal analysis conducted by Spearpoint et al. [13] the a term could be represented as:

$$\frac{MLR\ e}{\dot{q}''_{\text{inc}}} \approx a \approx \frac{(1-\tau_c)\ k_c\ (T_s - T_v)}{\Delta H_v\ \dot{q}''_{\text{inc}}}, \tag{7}$$

where k_c is the char conductivity, T_s and T_v are the surface and pyrolysis temperature, respectively, and ΔH_v is the heat of vaporization. Considering approximate values proposed by ref. [13] of k_c =0.06 W m^{-1} K^{-1}, $T_s - T_v$ =500 K and ΔH_v =0.94 kJ g^{-1} this coefficient would in the order of $a \approx 0.33$ g mm kJ^{-1}, which is coherent in order of magnitude to the coefficients fitted in Eq. 5. The expression proposed by Spearpoint also suggests that this term $\frac{MLR \times e}{\dot{q}''_{\text{inc}}}$ is not independent on the incident heat flux, which was not observed experimentally, as illustrated in Fig. 13. It is important to notice that all values are highly approximate, and the objective of this comparative analysis is to identity some key parameters that control the MLR of a given incident flux.

It seems nevertheless reasonable to assume that MLR is directly proportional to $\dot{q}''_{\text{inc}}$ for a given char front position, as suggested in this work (Eq. 4). The formulation expressed in ref. [13] suggests that, for a given char front position, MLR should be constant and independent of the heat flux. This latter formulation, constructed for qualitative analysis purposes, might not be accurate enough in order to quantify the relationships between MLR and char front position.

5.2 Limitations

This work proposes an engineering approach for the development of an expression for the mass loss rate under a cone calorimeter. This expression is entirely empirical and, as such, some limitations must be mentioned:

1. As of now, the model's validity in the range of 90-150 kW m^{-2}, which can occur in some fire scenarios, has not been tested.
2. As discussed in section. 5.1, no direct explanation is yet provided for the discrepancies between the measured MLR^* values and the theoretical solution shown in Eq. 7, taken from [13]. The dependence of the incident heat flux on MLR^* and negligible permanent regime term were factors that diverged from the data observation by our experimental team. Their possible origins were briefly discussed in section. 5.1.
3. The real burning behavior in the transient peak regime is far more complex than in the steady state regime. Many heat and mass transfer mechanisms seem to influence the outcome of material mass loss. The correlation is purely empirical and, particularly for the low values of the char front position, may be inaccurate. For fire safety engineering applications, this limitation could be overcome by majoring the correlation law with respect to the observed standard deviation over the whole experimental setup.
4. The correction of the incident heat flux by a complementary heat source contribution was promising but exploratory, especially for smoldering combustion. Understanding this phenomenon for other heat fluxes and oxygen content conditions is a major perspective of this work. A difficulty in implementing this expression in a flame spread model is the detection of flaming or smoldering combustion, and the calculation of the resulting heat sources. [26]. The transient peak regime also shows a significant discrepancy with experimental data for the lowest heat fluxes, where no visible flame was detected [20]. It seems that the flame heat flux in contact with the virgin wood plays an important role in this phase. This is evidenced by comparison with the experimental curves at $\dot{q}''_{\text{cone}} = 38.5$ and 49.5 kW m^{-2} shown in Fig. 3.
5. As shown in Fig. 11(a) for the cases of $\dot{q}''_{\text{cone}} = 82.5$ and 93.5 kW m^{-2} the correlation over-predicts the MLR as the thermally thick assumption is no longer valid, i.e., when the wood is almost entirely carbonized. The opposite effect has also been reported to occur, i.e., the burning rate increases at the end of the test when the pyrolysis zone reaches the rear side of the sample [37]. As a consequence, the approach proposed in this work could also lead to an under-prediction of the MLR in these cases. This effect is not considered by the proposed correlation and further investigation is required.
6. Finally, this expression has been tested so far under relatively simple conditions: bench-scale gasification tests, vertical orientation and constant heat fluxes. Another perspective of this work is the implementation of this expression in larger-scale calorimetry experiments, different charring materials and other ambient conditions. In particular, non-constant incident heat flux should be considered in order to extend the validity of the correlation.

6 Conclusion

This article presents the development of an empirical expression that describes the degradation of spruce wood in bench-scale gasification experiments for a wide range of incident heat fluxes. The presented correlation allows prediction of the material mass loss rate as a function of the heat flux with minimal input of material properties and calibration. The experimental procedure was first presented. Then, a treatment of the cone calorimeter data that allowed the development of the correlation was described. A comparison with theoretical thermal analysis of wood degradation from the literature was drawn, and the limitations of this approach were finally discussed.

Samples of spruce wood in the form of glue-laminated timber were exposed to a cone radiant heater providing a constant heat flux ranging from $\dot{q}''_{\text{cone}} = 22$ to 93.5 kW m^{-2}. The mass loss rate per unit area (MLR), char front position and a preliminary smoldering combustion heat source were experimentally determined.

An experimental treatment of the MLR was proposed, consisting of normalizing the MLR by the heat flux and depicting it as a function of the char front position. This procedure resulted in a grouping of the experimental curves in the x and y axis, thus allowing the development of a generalized expression that predicts the MLR for whatever constant heat flux within engineering accuracy. This generalized expression could be ultimately used as a constitutive relation for wood degradation prediction.

A comparison with a theoretical thermal analysis of wood burning from the literature was then performed. The MLR normalized by the heat flux was not dependent on the heat flux as the theoretical analysis suggested. A permanent regime was also added to the empirical correlation to account for continuous material pyrolysis as the char front position increases, which was experimentally observed. The factors that could contribute to this discrepancy were briefly discussed.

This pyrolysis modeling approach has been recently implemented in the CFD fire modeling package Fire Dynamics Simulator (FDS) [33, 34]. The robustness of this approach, named S-pyro, was evaluated using bench-scale data for 149 different materials, from 6 distinct public datasets [38]. Only a mathematical model is proposed in it, however. It consists of the scaling of the burning rate in X and Y axis, extrapolating the HRR outcome over time from a single reference heat flux. This manuscript complements the mathematical model by providing a novel physical interpretation to this formulation, relating the behavior of the burning rate to the char layer depth.

The same approach as used in this work could be implemented with a focus on the determination of the charring rate of timber. It could be particularly useful for the study of structural analysis under heat exposure. These applications will be also explored in a future work. This work is however entirely empirical and thus the limitations of this expression were identified. The elements that correlate the heat flux to the mass loss rate are still not well understood in a thermal analysis point of view. More physically-based discussions and the investigation of this behavior for other tests and materials are considered as perspectives for future works.

References

[1] Wiesner, F., Bisby, L.: The structural capacity of laminated timber compression

elements in fire: A meta-analysis. Fire Safety Journal **107**, 114–125 (2019)

[2] Zachar, M., Mitterová, I., Xu, Q., Majlingová, A., Cong, J., Galla, Š., *et al.*: Determination of fire and burning properties of spruce wood. Drvna industrija **63**(3), 217–223 (2012)

[3] Terrei, L., Acem, Z., Georges, V., Lardet, P., Boulet, P., Parent, G.: Experimental tools applied to ignition study of spruce wood under cone calorimeter. Fire Safety Journal **108**, 102845 (2019)

[4] White, R., Dietenberger, M.: Fire safety. wood handbook—wood as an engineering material. Gen. Tech. Rep. FPL-GTR-113. Madison: US Department of Agriculture, Forest Service, Forest Products Laboratory (1999)

[5] Maciulaitis, R., Lipinskas, D., Lukosius, K.: Singularity and importance of determination of wood charring rate in fire investigation. Materials Science **12**(1), 42–47 (2006)

[6] Njankouo, J.M., Dotreppe, J.-C., Franssen, J.-M.: Experimental study of the charring rate of tropical hardwoods. Fire and materials **28**(1), 15–24 (2004)

[7] Lizhong, Y., Zaifu, G., Yupeng, Z., Weicheng, F.: The influence of different external heating ways on pyrolysis and spontaneous ignition of some woods. Journal of Analytical and Applied Pyrolysis **78**(1), 40–45 (2007)

[8] Di Blasi, C.: Numerical simulation of cellulose pyrolysis. Biomass and Bioenergy **7**(1-6), 87–98 (1994)

[9] Sinha, S., Jhalani, A., Ravi, M., Ray, A.: Modelling of pyrolysis in wood: a review. SESI Journal **10**(1), 41–62 (2000)

[10] Janssens, M.L.: Modeling of the thermal degradation of structural wood members exposed to fire. Fire and materials **28**(2-4), 199–207 (2004)

[11] Bamford, C., Crank, J., Malan, D.: The combustion of wood. part i. In: Mathematical Proceedings of the Cambridge Philosophical Society, vol. 42, pp. 166–182 (1946). Cambridge University Press

[12] Kanury, A.M.: Burning of wood—a pure transient conduction model. Journal of Fire and Flammability **2**(3), 191–205 (1971)

[13] Spearpoint, M., Quintiere, J.: Predicting the burning of wood using an integral model. Combustion and flame **123**(3), 308–325 (2000)

[14] Lautenberger, C., Fernandez-Pello, C.: A model for the oxidative pyrolysis of wood. Combustion and Flame **156**(8), 1503–1513 (2009)

[15] Hostikka, S., Matala, A.: Pyrolysis model for predicting the heat release rate of

birch wood. Combustion Science and Technology **189**(8), 1373–1393 (2017)

[16] Richter, F., Rein, G.: A multiscale model of wood pyrolysis in fire to study the roles of chemistry and heat transfer at the mesoscale. Combustion and Flame **216**, 316–325 (2020)

[17] Kim, M., Dembsey, N.: Parameter estimation for comprehensive pyrolysis modeling: Guidance and critical observations. Fire Technology **51**, 443–477 (2015)

[18] Tran, H.C., White, R.H.: Burning rate of solid wood measured in a heat release rate calorimeter. Fire and materials **16**(4), 197–206 (1992)

[19] Girardin, B., Duny, M., Dréan, V., Auguin, G.: Assessment of an engineering method for the contribution of wood: Application to iso 9705 with different linings coverage. Interflam 2019 (2019)

[20] Terrei, L.: Comportement au feu du matériau bois: auto-inflammation, dégradation et auto-extinction. PhD thesis, Université de Lorraine (2020)

[21] Terrei, L., Acem, Z., Marchetti, V., Lardet, P., Boulet, P., Parent, G.: In-depth wood temperature measurement using embedded thin wire thermocouples in cone calorimeter tests. International Journal of Thermal Sciences **162**, 106686 (2021)

[22] ISO 5660-1:2015: Reaction-to-fire Tests — Heat Release, Smoke Production and Mass Loss Rate — Part 1: Heat Release Rate (cone Calorimeter Method) and Smoke Production Rate (dynamic Measurement), p. 55 (2015). https://www.iso.org/standard/57957.html

[23] Friquin, K.L.: Material properties and external factors influencing the charring rate of solid wood and glue-laminated timber. Fire and materials **35**(5), 303–327 (2011)

[24] Lizhong, Y., Yupeng, Z., Yafei, W., Zaifu, G.: Predicting charring rate of woods exposed to time-increasing and constant heat fluxes. Journal of Analytical and Applied Pyrolysis **81**(1), 1–6 (2008)

[25] Boonmee, N., Quintiere, J.: Glowing and flaming autoignition of wood. Proceedings of the combustion institute **29**(1), 289–296 (2002)

[26] Morrisset, D., Hadden, R.M., Bartlett, A.I., Law, A., Emberley, R.: Time dependent contribution of char oxidation and flame heat feedback on the mass loss rate of timber. Fire Safety Journal **120**, 103058 (2021)

[27] Babrauskas, V.: Charring rate of wood as a tool for fire investigations. Fire Safety Journal **40**(6), 528–554 (2005)

[28] Quintiere, J.G.: A semi-quantitative model for the burning rate of solid materials. National Inst. of Standards and Technology (BFRL), Gaithersburg, MD (United

States) (1992)

[29] Lyon, R.E.: Solid-state thermochemistry of flaming combustion. Marcel Dekker, Inc., NY (2000)

[30] Gray, M.R., Corcoran, W.H., Gavalas, G.R.: Pyrolysis of a wood-derived material. effects of moisture and ash content. Industrial & Engineering Chemistry Process Design and Development **24**(3), 646–651 (1985)

[31] Bartlett, A., Hadden, R., Bisby, L., Law, A.: Analysis of cross-laminated timber charring rates upon exposure to non-standard heating conditions. Fire Mater, 667–681 (2015)

[32] Martinka, J., Rantuch, P., Liner, M.: Calculation of charring rate and char depth of spruce and pine wood from mass loss. Journal of Thermal Analysis and Calorimetry **132**, 1105–1113 (2018)

[33] McGrattan, K., McDermott, R., Vanella, M., Mueller, E.: Fire dynamics simulator user's guide. NIST Special Publication 1019 Sixth Edition (2023)

[34] McGrattan, K., Hostikka, S., Floyd, J., McDermott, R., Vanella, M., Mueller, E.: Fire dynamics simulator technical reference guide volume 1: Mathematical model. NIST Special Publication 1018-1 Sixth Edition (2023)

[35] Harada, T.: Time to ignition, heat release rate and fire endurance time of wood in cone calorimeter test. Fire and materials **25**(4), 161–167 (2001)

[36] Li, K., Hostikka, S., Dai, P., Li, Y., Zhang, H., Ji, J.: Charring shrinkage and cracking of fir during pyrolysis in an inert atmosphere and at different ambient pressures. Proceedings of the Combustion Institute **36**(2), 3185–3194 (2017)

[37] Sanned, E., Mensah, R.A., Försth, M., Das, O.: The curious case of the second/end peak in the heat release rate of wood: A cone calorimeter investigation. Fire and Materials (2022)

[38] Hodges, J.L., Lattimer, B.Y., Kapahi, A., Floyd, J.E.: An engineering model for the pyrolysis of materials. Fire safety journal **141**, 103980 (2023)

7 Annex

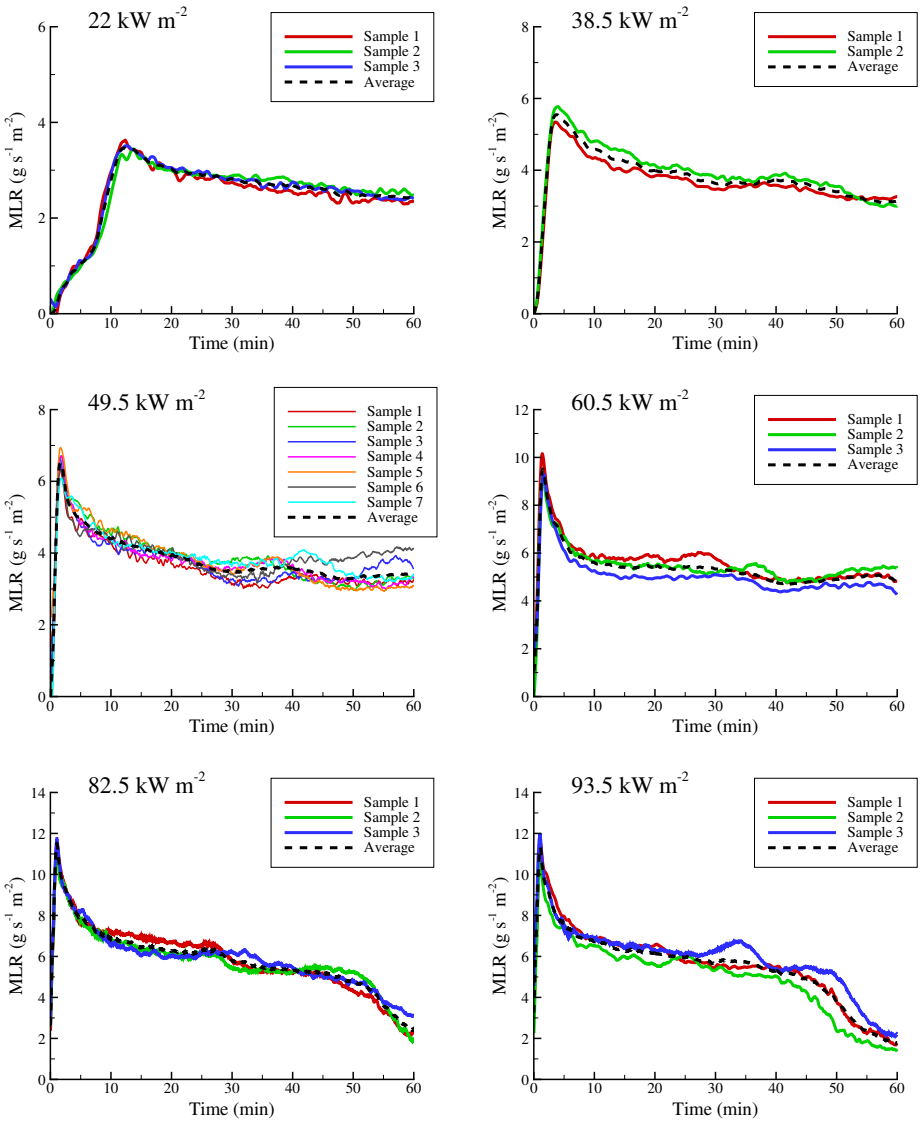

Fig. 14 Unfiltered individual MLR data for each full experimental test.